Bulletin of the Seismological Society of America, Vol. 79, No. 4, pp. 1177–1193, August 1989

AN ALGORITHM FOR AUTOMATED TSUNAMI WARNING IN FRENCH POLYNESIA BASED ON MANTLE MAGNITUDES

BY JACQUES TALANDIER AND EMILE A. OKAL

ABSTRACT

We have developed a new magnitude scale, M_m, based on the measurement of mantle Rayleigh-wave energy in the 50 to 300 sec period range, and directly related to the seismic moment through $M_m = \log_{10}M_0 - 20$. Measurements are taken on the first passage of Rayleigh waves, recorded on-scale on broadband instruments with adequate dynamical range. This allows estimation of the moment of an event within minutes of the arrival of the Rayleigh wave, and with a standard deviation of ±0.2 magnitude units. In turn, the knowledge of the seismic moment allows computation of an estimate of the high-seas amplitude of a range of expectable tsunami heights. The latter, combined with complementary data from *T*-wave duration and historical references, have been integrated into an automated procedure of tsunami warning by the Centre Polynésien de Prévention des Tsunamis (CPPT), in Papeete, Tahiti.

INTRODUCTION

The goal of the present paper is to report on a method which we have developed to determine in real time the seismic moment of a distant earthquake and an estimate of its tsunami risk, based on a one-station analysis of mantle Rayleigh waves recorded on broadband instruments offering satisfactory response characteristics well into the low-frequency seismic range of the spectrum. This method lends itself well to automation, and, combined with automatic event detection and location, has been implemented since November 1987 at the Centre Polynésien de Prévention des Tsunamis (CPPT) operated by the Geophysical Laboratory in Papeete, Tahiti.

Background

The need to protect life and property in coastal areas from the devastating effects of tsunamis is obvious. For tsunamis generated at sufficiently large distances from a receiving shore, the relatively slow nature of their propagation holds the intrinsic *a priori* possibility of an adequate warning (to be followed if necessary by evacuation), which must rely on an accurate scientific interpretation of the tsunamigenic potential of the parent earthquake. This area has been the subject of intense research over the past few decades.

This paper is not concerned with effects such as the so-called "run-up," which amplifies the wave in shallow water, and resonance due to the particular shape of bays and harbors; the latter can be successfully modeled through computational techniques, such as finite-element codes, given an adequate model of coastal bathymetry. Rather, we focus on what amounts to the seismological input (as a space-time boundary condition) to such calculations, namely the relationship between the parent earthquake and the amplitude of the tsunami on the high seas, prior to the initiation of run-up.

The Importance of the Seismic Moment M_0

About 20 yr ago, Aki (1967) introduced the seismic moment M_0 as a physical measurement of the "size" of an earthquake, and later Kanamori (1972) and Abe

(1973) identified M_0 of the parent earthquake as the major factor controlling tsunami generation. This observation illustrates the fact that the tsunami can be considered as a particular case of seismic wave: because of the finite rigidity of the Earth, the tsunami eigenfunction penetrates the solid Earth, where its energy is mostly elastic (as opposed to gravitational in the oceanic layers). As such, this continuation of the tsunami wave into the Earth, although of very small amplitude, can be excited by an earthquake source. We refer to Ward (1980) for an application of the general formalism of normal mode theory to the case of tsunami excitation, and to Okal (1988) for a discussion of the "pseudo-Rayleigh" wave continuing the tsunami eigenfunction into the solid Earth, under various conditions of coupling between ocean and hard rock, including in the presence of sediments. An important, if somewhat surprising, result of our previous study (Okal, 1988) was that the effect on tsunami excitation of such factors as focal geometry and precise hypocentral depth is to a large extent secondary. This derives directly from the description of tsunami excitation in the framework of seismic source theory and, as far as depth is concerned, from the very large wavelengths involved, which result in a slow decay of the pseudo-Rayleigh wave with depth inside the solid Earth.

Figure 1 gives an example of the linear correlation between seismic moment and tsunami amplitude (in this case at Papeete, Tahiti, where run-up and resonance effects are minimal). That the static seismic moment (ideally measured at zero-frequency) should control the excitation of tsunamis further expresses their very low-frequency character, with most of their energy typically concentrated around 1 mHz.

A practical consequence of our theoretical results is that the accurate resolution of the focal geometry of an earthquake and of its hypocentral depth is not of prime necessity in the assessment of its tsunamigenic character, and may even be a waste

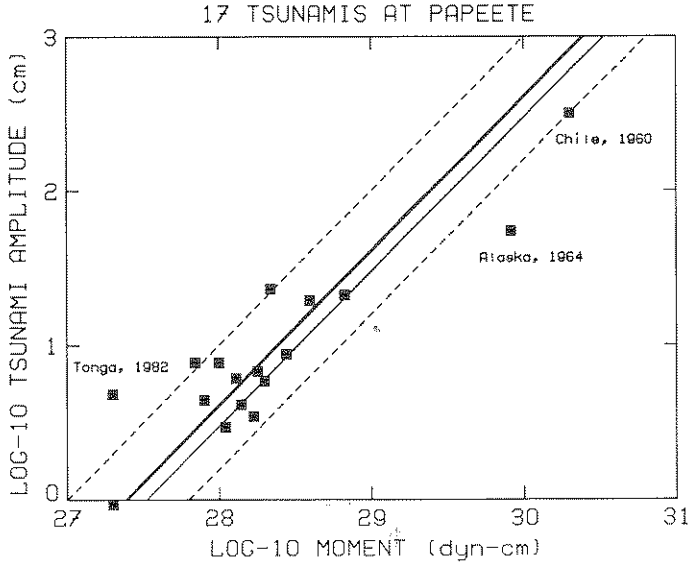

FIG. 1. Peak-to-peak equalized tsunami amplitude (TS^e) vs. seismic moment of the parent earthquake, for 17 tsunamis recorded at PPT (1958 to 1986). The thin solid line is the theoretical relation (6); the thick line the linear relation (8), best-fitting the dataset under the constraint of a slope of 1; the dashed lines are the upper and lower bounds, (9) and (11), respectively. The individual events discussed in the text, notably those two not fitting within these bounds are identified.

of time and resources under operational real-time conditions. Rather, we seek a one-station estimate of the earthquake's moment, irrespective of depth and geometry: such a measurement follows the philosophy of the *magnitude* concept.

Figure 1 illustrates that very large seismic sources (typically $M_0 \geqq 10^{28}$ dyne-cm) are required to generate significant, and *a fortiori* damaging, tsunamis. However, in this range of earthquake size, it has long been known that any magnitude scale measured at a constant period T, such as the standard body- and surface-wave magnitudes m_b and M_s, saturates when the duration of rupture along the fault becomes comparable to T (1 sec for m_b, 20 sec for M_s) (Kanamori and Anderson, 1975a; Geller, 1976). Since m_b and M_s then cease to provide an adequate representation of the true "size" of the earthquake source, these magnitude scales must be considered useless for accurate tsunami warning, and their use can lead to failures and false alarms, both of which are highly undesirable from a social standpoint.

On the other hand, M_0 measured at least in principle at zero-frequency, keeps growing with earthquake size, rather than saturating. For this reason, the real-time measurement of the seismic moment M_0 remains a primary goal of observational seismology.

The Difficulty of Measuring M_0 in Real Time

Measurements of M_0 are usually made through multi-station moment-tensor inversion of either surface waves or body waves (Dziewonski and Woodhouse, 1983; Romanowicz and Guillemant, 1984). Most of the body-wave energy is concentrated at periods not exceeding 40 sec, and a moment estimate obtained from body waves may not be accurate at the ultra-low frequencies of interest for tsunami generation. On the other hand, surface-wave moment-tensor inversion uses energy typically in the 150 to 300 sec period range, which clearly leads to a more adequate representation of the static moment. However, many presently available digital instruments saturate, clip, or otherwise behave nonlinearly, during the first passage of surface waves for truly large events; most moment-tensor solutions for such earthquakes have been obtained from subsequent passages (R_2, R_3, etc.). Even in the ideal world of instant satellite telecommunications, this has the obvious inconvenient of delaying the computation of an estimate of M_0 by several hours, an interval of time that may become crucial should evacuation of low-lying areas be warranted. This is especially true at short epicentral distances (e.g., in the Tonga-to-Tahiti geometry).

Since the early 1960s, CPPT had used the duration of T waves propagating in the ocean's SOFAR channel as a means of obtaining in real time an estimate of the dimension of the faulting area in the epicentral region. We refer to Talandier (1966, 1972) and Okal and Talandier (1986) for a discussion of this method, and of its theoretical basis. It is clear, however, that Rayleigh waves, representative of the low-frequency energy radiated by the event, can provide a better (and quicker) estimate of M_0.

A major improvement in this respect has come in the past few years with the development of broadband instruments offering a basically flat response well into the frequency range characteristic of very-long-period seismology. In particular, it is now possible to routinely obtain high quality records of the first passage R_1 of ultra-long-period Rayleigh waves in the 100 to 300 sec period range, even from the largest teleseismic events. An example of such records is given in Figure 2. There are several advantages to the use of R_1 as opposed to subsequent passages. First, and because of its shorter travel time, R_1 is less affected by lateral heterogeneity, and has been shown to be more reliable for the retrieval of earthquake source

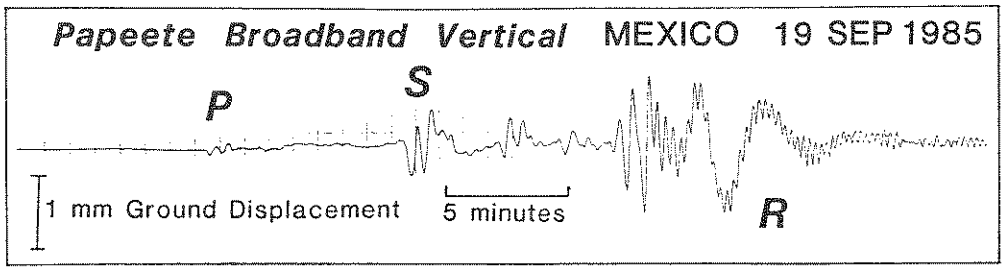

FIG. 2. Papeete broadband record of the Mexican earthquake of 19 September 1985.

parameters (Monfret and Romanowicz, 1986). Also, and again simply because it arrives sooner, R_1 has the potential for the earlier issuance of a tsunami watch or warning. This opens the door to a real-time, single-station measurement of the seismic moment, using the first passage of Rayleigh waves. The development of such a technique, leading to a "mantle" magnitude M_m measured at very long periods, is the subject of our research.

THE MANTLE MAGNITUDE M_m

In this section, we discuss the principal features of a new magnitude scale, M_m, which we have recently developed in order to obtain reliable real-time estimates of seismic moments. Its key ingredient is the use of a *variable* period guarding against the effects of saturation, as the size of the event keeps growing. A full description and justification of M_m is given in Okal and Talandier (1989). In the present paper, we only review rapidly the various terms used in its calculation. We then give experimental results from the broadband station at Papeete, Tahiti, and describe the resulting estimation of the tsunami risk as a function of M_m and the automation of the method.

In the present endeavor, we are driven by several goals: first, retrieval of the seismic moment M_0, and second, retention of the concept of magnitude, with its direct relationship to the amplitude of ground motion. We refer to Okal and Talandier (1987, 1989) for specific details on the theoretical background of our proposed formulas. Specifically, we define M_m as

$$M_m = \log_{10} M_0 - 20 \tag{1}$$

where M_0 is in dyne-cm. The *ad hoc* constant 20 provides a simple link between M_m and M_0 and keeps M_m values in the general range of conventional magnitudes. In this fashion, we impose a slope of 1 between M_m and $\log_{10} M_0$, which is a reflection of our use of variable, but sufficiently large periods, allowing us to stay below the corner frequency of the source, in a range where no saturation effects are present (Geller, 1976). Finally, in this study, we restrict ourselves to shallow sources ($h \leqq 75$ km), characteristic of large subduction zone events, and bearing substantial tsunami risk.

Theory

As discussed in detail in Okal and Talandier (1989), we base the development and measurement of M_m on the theory of excitation of normal modes and surface waves by seismic sources (Saito, 1967; Gilbert, 1971; Kanamori and Stewart, 1976). Following Harkrider (1964), we separate the effects of propagation from source excitation. The propagation terms depend only on distance and frequency; the

excitation terms depend only on seismic moment, frequency, depth, and focal mechanism. Accordingly, we use an expression of the form

$$\log_{10}M_0 = \log_{10}X(\omega) + C_D + C_S + C_0, \tag{2}$$

to recover the seismic moment from the amplitude spectrum of a Rayleigh wave. Here, $X(\omega)$ is the spectral amplitude at an angular frequency ω, C_D is a distance correction, C_S a source correction, and C_0 a constant. Equation (2) lays the ground for the definition of a magnitude scale at variable frequency.

Distance correction C_D

The correction is simply $C_D = 0.5 \log_{10}\sin\Delta + (\log_{10}e)\omega l_{\text{deg}}\Delta/2UQ$, where Δ is the epicentral distance in degrees and l_{deg} is the length of 1 degree (111.2 km). Both terms are independent of focal geometry and depth. The first one reflects geometrical spreading on the spherical Earth; the second one corrects for anelastic attenuation. In order to compute the latter, we use a model of the Earth regionalized into seven tectonic provinces along a $10° \times 10°$ coordinate grid (see Fig. 3). In each region, we use a different model for group velocity U and attenuation Q^{-1}. These models, listed on Table 1, are based upon the work of Canas and Mitchell (1978), Mitchell and Yu (1980), Nakanishi (1981), and Hwang and Mitchell (1987). The particular path under study is then split into segments sampling the various tectonic provinces, and their contributions to C_D added.

Source Correction C_S

The correction C_S is somewhat more complex and depends *a priori* on a combination of frequency, depth, and focal geometry. Since we do not seek the solution of the full moment tensor, but rather an estimate of the scalar moment, we assume

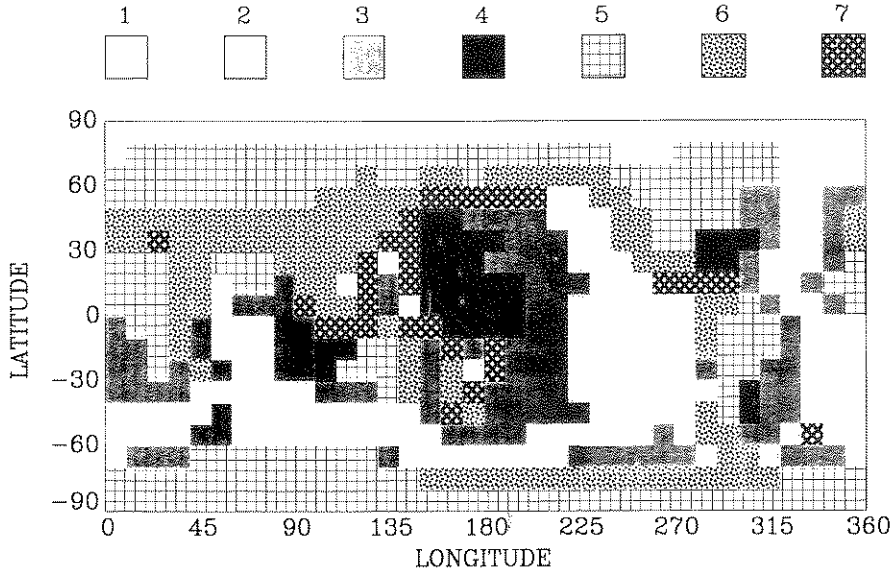

FIG. 3. Tectonic regionalization used in the computation of the distance correction C_D. The various shading patterns refer to oceans (1: less than 20 Ma; 2: 20 to 50 Ma: 3: 50 to 100 Ma; 4: older than 100 Ma); continents (5: shields; 6: tectonic regions); and trenches (7). See Table 1 for corresponding values of U and Q.

TABLE 1

REGIONALIZED DISPERSION AND ATTENUATION MODELS USED IN COMPUTING DISTANCE CORRECTION

T (sec)	Region 1 0–20 Ma		Region 2 20–50 Ma		Region 3 50–100 Ma		Region 4 > 100 Ma		Region 5 Shields		Region 6 Mountains		Region 7 Trenches	
	U (km/sec)	Q	U (km/sec)	Q	U (km/sec)	Q	U (km/sec)	Q	U (km/sec)	Q	U (km/sec)	Q	U (km/sec)	Q
35	3.845	158	4.005	168	4.046	200	4.013	251	3.455	236	2.950	98	2.880	96
38	3.836	152	3.995	162	4.061	191	4.040	234	3.536	220	3.070	95	2.900	90
42	3.819	147	3.976	155	4.063	181	4.064	217	3.634	204	3.170	92	2.920	85
46	3.799	143	3.953	150	4.055	173	4.074	204	3.722	192	3.250	90	2.940	82
51	3.772	139	3.927	145	4.043	166	4.073	191	3.818	181	3.300	92	2.960	79
56	3.746	136	3.899	140	4.023	159	4.062	183	3.858	177	3.380	94	2.980	78
63	3.714	133	3.863	136	3.992	153	4.037	175	3.899	181	3.520	96	3.000	79
70	3.690	131	3.831	134	3.958	149	4.007	169	3.920	179	3.560	98	3.040	80
78	3.670	129	3.799	132	3.919	145	3.972	166	3.936	192	3.620	100	3.070	81
87	3.657	129	3.770	131	3.879	143	3.934	165	3.954	212	3.690	103	3.100	82
90	3.649	130	3.743	132	3.836	142	3.893	166	3.952	251	3.710	106	3.130	84
111	3.642	133	3.718	134	3.794	144	3.850	170	3.928	260	3.700	109	3.170	87
127	3.632	138	3.694	140	3.753	148	3.806	177	3.896	295	3.680	112	3.218	92
145	3.617	146	3.671	149	3.715	155	3.761	188	3.854	333	3.700	116	3.419	99
167	3.590	159	3.643	161	3.673	168	3.710	203	3.797	280	3.780	120	3.515	108
193	3.554	177	3.611	180	3.631	187	3.657	222	3.743	250	3.580	125	3.623	119
223	3.524	201	3.586	204	3.601	209	3.617	245	3.666	283	3.550	130	3.526	131
259	3.541	231	3.606	234	3.620	239	3.628	272	3.645	312	3.470	155	3.475	149
300	3.669	262	3.727	266	3.742	271	3.745	297	3.706	345	3.610	200	3.699	170

that the focal geometry of the event is unknown and use a correction averaged over the orientation of the focal mechanism. We have shown in Okal and Talandier (1989) that the following expression

$$C_S = 1.6163\theta^3 - 0.83322\theta^2 + 0.42861\theta + 3.7411 \tag{3}$$

where $\theta = \log_{10} T - 1.8209$ (T in sec), gives an adequate source correction, to within ± 0.2 units of magnitude, in all cases when the focal mechanism is not "pure" (either pure horizontal or pure vertical slip on a pure vertical fault plane, with the station at a node of radiation), and for depths between 10 and 75 km. Equations (1) and (2) then yield:

$$M_m = \log_{10} X(\omega) + C_D + C_S - 0.90 \tag{4}$$

where $X(\omega)$ is in μm-sec.

MEASUREMENTS AT PAPEETE AND PERFORMANCE OF M_m

Instrumentation and Method

M_m measurements at Papeete, Tahiti (PPT) are taken on broadband records, available at the station since 1973. The instrumental response of the broadband system is flat in displacement from 1 sec to 150 sec and decreases by a factor of $\sqrt{2}$ at 300 sec. As discusssed in detail in Okal and Talandier (1989), we have compiled M_m values for 45 earthquakes, ranging in moments from 7.6×10^{25} to 1.8×10^{28} dyne-cm, and having occurred at distances ranging from 23 to 85°.

For each record, a 4096-point digital time series (with a sampling rate of 0.2 sec) is Fourier-transformed, and at each period $T = 2\pi/\omega \geqq 50$ sec, the spectral amplitude

$X(\omega)$ is retained. We then apply the distance and source corrections C_D and C_S. We keep the largest among the values of M_m computed at various frequencies. This procedure attempts to guard against the possibility of the station sitting in a node of Rayleigh-wave radiation at a particular period. Obviously, in the case of a "pure" geometry such as a strike-slip earthquake on a vertical fault, the azimuth of the nodes are frequency-independent; however, the shape of radiation patterns can be extremely dependent on frequency for focal geometries involving nonvertical faults and/or oblique slip. A change of reference period can literally move the station out of the node. Similarly, source finiteness can result in strong spectral holes beyond the corner frequency. By computing M_m at various periods and retaining its maximum value, one can hope to eliminate such problems and more precisely estimate the earthquake's moment.

Results

For this dataset of 45 earthquakes, the mean and standard deviation of the residual r between values of M_m computed from (1) and measured according to (4) are $\bar{r} = 0.02$; $\sigma = 0.18$ units of magnitude. The latter corresponds to an uncertainty of a multplicative or divisive factor f of 1.51 on the seismic moment (which we will write as $f = */1.51$). These results are also shown on Figure 4. We regard them as generally excellent. First, it should be remembered that individual estimates of seismic moments published by different investigators regularly show deviations on the order of $*/1.3$. Also, in the case of conventional magnitude scales (e.g., M_s at 20 sec), few single seismic stations can boast of having a systematic magnitude bias of less than 0.2 units, and a standard deviation also less than 0.2 units. In Talandier

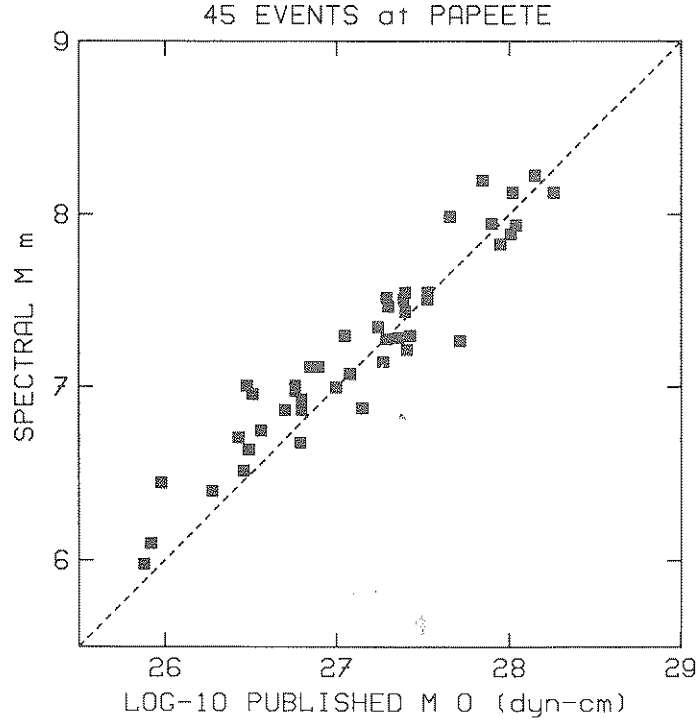

FIG. 4. Plot of spectral measurements of M_m, obtained through (4), against published values of M_0. The dashed line is the theoretical relation (1).

et al. (1987), we further proved that this method could not be improved by attempts to include a "source finiteness" correction, expressing the possible effects of source duration on the measured values of M_m. As a result, we believe that equation (4) provides a satisfactory means of computing M_0.

In Okal and Talandier (1989), we extended the concept of M_m to other stations by considering an additional 42 records on the ultra-long-period vertical instrument at Pasadena, and 169 records taken from various stations of the GEOSCOPE network. This extensive dataset was used in a series of tests, in an unsuccessful search for any possible bias of the measurements with either period, distance, or individual station. Our most important results were 1) that "station corrections" are not warranted, 2) that the method works well even at distances as short as 8°, and 3) that the influence of the procedure of ignoring focal geometry and depth in computing the source correction (3) degrades the goodness-of-fit by only 30 per cent.

Time-Domain Measurements

It has long been known that there exists a theoretical relationship between M_0 and the spectral amplitude $X(\omega)$ of a Rayleigh wave; however most magnitude measurements have traditionally been taken in the time domain. On the basis of the strong inverse dispersion of Rayleigh waves in the 50 to 250 sec period range, Okal and Talandier (1987) discussed a relationship of the form $X(\omega) = \frac{1}{2}\, a \cdot T$ where a is the zero-to-peak amplitude of a time-domain oscillation of period T, within a strongly dispersed wave train; its theoretical justification, based on phase-stationary asymptotics, is given in Okal (1989). This in turn suggests the direct measurement of M_m in the time domain using

$$M_m{}^{TD} = \log_{10}(a \cdot T) + C_D + C_S - 1.20 \tag{5}$$

where a is in microns, and T in seconds (if a peak-to-peak measurement is taken, the constant in (5) should be −1.50). For the purpose of tsunami warning at Papeete, we have to consider only distances less than 120°, for which (5) is accurate to within ±0.2 units of magnitude, as long as $T \leqq 200$ sec. At greater distances, and in particular for multiple Rayleigh passages, the additional distance correction $0.5 \log_{10}(\Delta/70)$ would be warranted.

The possibility of directly obtaining M_m in the time domain was tested by measuring the amplitudes and periods of the arches making up dispersed Rayleigh waves, and retaining the largest value of $M_m{}^{TD}$ computed through (5). As described below, this procedure lends itself well to automation. We have measured $M_m{}^{TD}$ according to equation (5) for 45 earthquakes, resulting in $\bar{r} = -0.07$, $f = */1.60$. This excellent agreement between computed and measured values upholds the concept of a mantle magnitude, measured directly in the time domain.

As shown by Talandier *et al.* (1987), it is also possible to extend the concept of a time-domain measurement of the magnitude M_m to lower seismic moments. In this case, we found a residual $\bar{r} = 0.15$, $f = */1.57$ for a dataset of 88 earthquakes extending down to $M_m = 4.5$. Although this does not bear directly on tsunami prevention, we consider it important, since it proves the universality of the new magnitude scale. It should not be surprising that a good fit can be obtained between the time-domain visual measurements of M_m and $\log_{10} M_0$ for the smaller events, since this is simply an example of the relationship between moment and magnitude in the absence of saturation effects (although the accuracy of C_S for the smaller

events, most of which involve measurements at periods between 20 and 35 sec, could be questionable). It is remarkable however that the same "locking" constants can be used in equation (5) over four orders of magnitudes, and with periods ranging from 20 to 200 sec. This character of universality at all periods is the most important and promising feature of the mantle magnitude scale M_m.

Estimation of Tsunami Risk and Warning Procedures

Once a seismic moment is computed through the measurement of the magnitude M_m, an estimate of tsunami risk can be evaluated using the flow chart on Figure 5. The most important ingredient to this procedure is the proportionality of observed tsunami heights to the seismic moment.

From Moment to Tsunami Height: Theoretical Marigrams

In order to study accurately the dependence of tsunami amplitude with distance, we have computed a series of synthetic marigrams at distances ranging from 5° to 175°. As described in detail in Okal (1989), we use a variation of normal mode

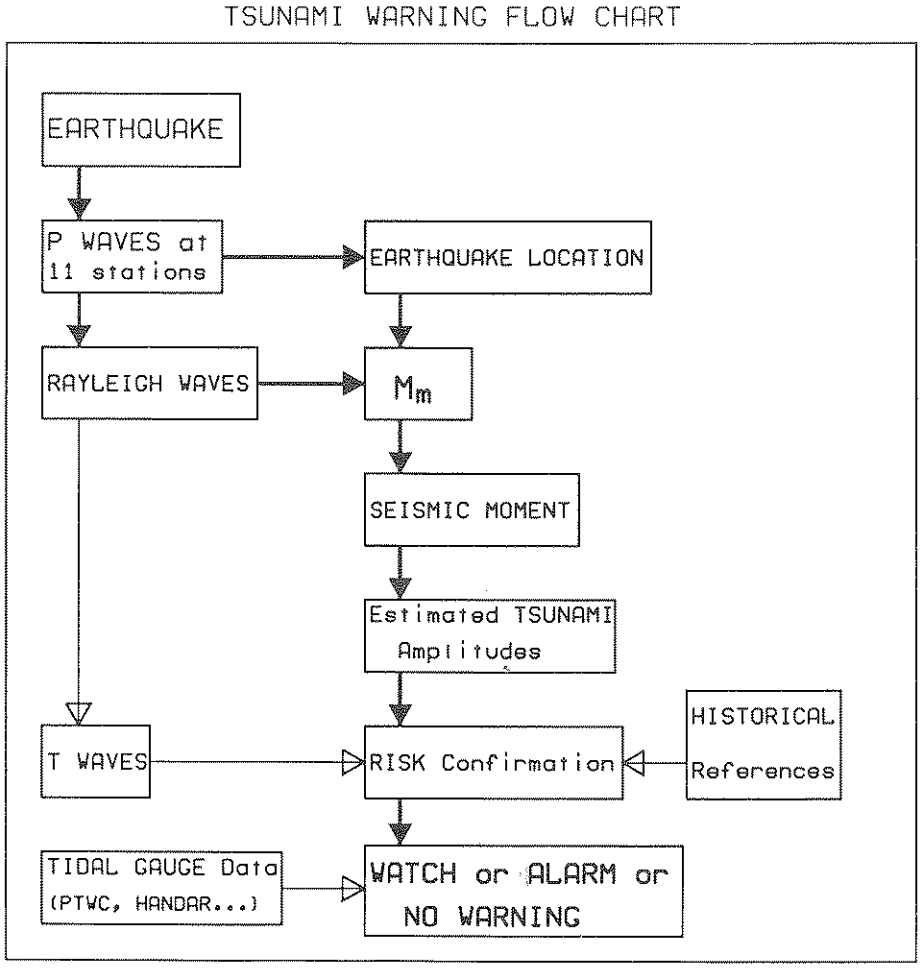

FIG. 5. Flow chart of tsunami warning organization at PPT. The thinner traces involving T waves and historical references indicate the complementary nature of these ingredients.

theory, introduced by Ward (1980). We chose a hypocentral depth of 20 km and a pure thrust-faulting mechanism on a 45°-dipping fault (the so-called "T45" geometry in the notation of Okal (1988)). We located the station at the maximum of radiation, i.e., 90° from the strike of the fault plane. The solid line on Figure 6a shows the variation of the amplitude of the resulting amplitude as a function of distance. The peak-to-peak tsunami amplitude can be modeled as

$$TS = 0.3M_0 \frac{1}{\sqrt{\sin \Delta}} \sqrt{\frac{90}{\Delta}} \tag{6}$$

where TS is in cm, Δ in degrees, and M_0 in units of 10^{27} dyne-cm. This curve is shown as the dashed line on Figure 6a. Both terms in this expression are readily explained: the first one represents the geometrical spreading of the tsunami wave on the sphere; the second one is due to the slight dispersion of the tsunami wave with frequency, and can be derived mathematically from phase-stationary asymptotics (Erdélyi, 1956; Okal, 1989). This approximation is expected to break down at short distance, for which dispersion is unsufficient; it is clear on Figure 6 that the two curves separate at short distances, but Figure 6b shows that the modeling of the tsunami amplitude by (6) does not entice errors greater than 10 per cent in amplitude at distances greater than 15°.

Comparison with Data at Papeete

On Figure 1, the peak-to-peak amplitudes of the 17 tsunamis recorded at Papeete since 1958 have been equalized to a common distance of 90° through multiplication by a factor $\sqrt{(\Delta \sin \Delta)/90}$. The light solid trace is the theoretical tsunami amplitude expected from (6) and the published value of the seismic moment, as listed in Table 2. In general, we find excellent agreement between the theoretical and expected values. This illustrates the fact that focal geometry plays little role in tsunami excitation (Okal, 1988), and further that run-up and resonance at Papeete are minimal. The best-fitting straight line through the dataset is

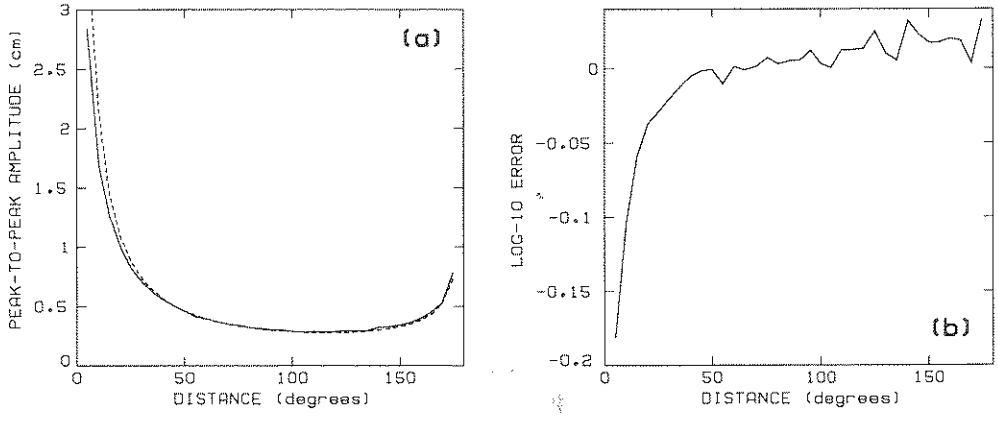

FIG. 6. Theoretical peak-to-peak tsunami amplitude as a function of distance. (*a*): The full trace results from normal mode summation carried out at distance increments of 5°. The dashed line is the result of modeling according to (6), and for a moment of 10^{27} dyne-cm. (*b*): Plotted is the decimal logarithm of the error involved when modeling the tsunami height by (6), taken as the ratio of the two curves in (*a*). Note that except at very short distances, it is usually less than 0.1 magnitude units, and therefore negligible.

$$\log_{10}M_0 = (1.22 \pm 0.12)\log_{10}(TS^e) + 27.17 \quad (7)$$

(the superscript e denoting an amplitude equalized to 90°. Since the slope is not significantly different from 1, it can be constrained to this theoretical value, yielding

$$\log_{10}(TS^e) = \log_{10}M_0 - 27.39. \quad (8)$$

Figure 1 shows that for 15 out of the 17 data points, this relationship correctly predicts the tsunami height if the constant in (8) is allowed to range between 27.0 and 27.8. The other two cases are the Alaska earthquake of 28 March 1964, and the Tonga earthquake of 19 December 1982. The former shows a significant deficiency in its tsunami height, resulting from a strong directivity effect at the source, due to the exceptional geometry of the plate boundary in this part of the Pacific rim (Okal, 1988). The latter case is an example of a so-called "tsunami earthquake" (Kanamori, 1972; Fukao, 1979), for which the tsunami is much more intense than expected from the seismic moment (in this case by a factor of 8). Source complexity has been suggested for this event (Christensen and Lay, 1988). A recent study, however, has shown that the earthquake can be modeled as a simple pulse if the dipping of the ocean floor is taken into account, and that the rupture possibly reached the ocean floor, thus involving seismic release in a sedimentary layer and enhanced tsunami excitation (Okal, 1988; Lundgren *et al.*, 1988). In the case of the 1960 Chilean earthquake, the slight deficiency in tsunami amplitude could be due to a defocusing effect caused by the heterogeneity in ocean depths, and hence in tsunami velocities (Woods and Okal, 1987).

TABLE 2

TSUNAMI DATASET AT PAPEETE, 1958–1986

Date	Region	Distance to PPT (°)	Published Moment		Peak-to-peak amplitude (cm) at PPT	
			10^{27} dyne-cm	Reference	measured (TS)	equalized (TS^e)
06 Nov 1958	Kuriles	85.3	40	a	20	19
22 May 1960	Chile	67.6	2000	b	380	316
13 Oct 1963	Kuriles	83.2	67	c	22	21
28 Mar 1964	Alaska	78.6	820	d	59	55
17 Oct 1966	Peru	68.7	20	e	7	6
16 May 1968	Japan	85.9	28	f	9	9
11 Aug 1969	Kuriles	83.8	22	a	24	23
17 Jun 1973	Japan	84.7	7	g	8	8
03 Oct 1974	Peru	69.2	18	h	8	7
22 Jun 1977	Tonga	25.2	14	i	12	4
12 Dec 1979	Colombia	71.6	17	j	4	3
01 Sep 1981	Samoa	22.7	2	k	3	1
19 Dec 1982	Tonga	25.3	2	l, m	14	5
03 Mar 1985	Chile	70.5	10	n	9	8
19 Sep 1985	Mexico	58.4	11	o	4	3
07 May 1986	Aleutian	72.3	13	p	7	6
20 Oct 1986	Kermadec	27.0	8	m, q, r	12	4

References to published moments: a: Kanamori (1977); b: Kanamori and Anderson (1975b); c: Kanamori (1970a); d: Kanamori (1970b); e: Abe (1972); f: Kanamori (1971); g: Shimazaki (1974); h: Dewey and Spence (1979); i: Lundgren and Okal (1988); j: Dziewonski *et al.* (1987a); k: Dziewonski *et al.* (1988); l: Dziewonski *et al.* (1983); m: Lundgren *et al.* (1989); n: Dziewonski *et al.* (1985); o: Dziewonski *et al.* (1986); p: Dziewonski *et al.* (1987b); q: Dziewonski *et al.* (1987c); r: Romanowicz and Monfret [personal comm., 1987].

Finally, the difference of 0.13 magnitude units between the experimental constant 27.39 in (8), and the constant expected (27.52) from the theoretical relation (6) can be ascribed to the combined effects of departure from the average focal mechanism assumed in (6), and run-up and resonance at Papeete harbor. Its extremely small value is an illustration of the power of the method.

On the basis of the above dataset, we define a window of expected peak-to-peak tsunami amplitudes, as a function of seismic moment and distance:

$$\text{Upper bound:} \quad \log_{10}(TS)_{\text{max.}} = \log_{10}M_0 - 0.5\log_{10}(\Delta \sin \Delta) - 26.0 \qquad (9)$$

$$\text{Average:} \quad \log_{10}(TS)_{\text{aver.}} = \log_{10}M_0 - 0.5\log_{10}(\Delta \sin \Delta) - 26.4 \qquad (10)$$

$$\text{Lower bound:} \quad \log_{10}(TS)_{\text{min.}} = \log_{10}M_0 - 0.5\log_{10}(\Delta \sin \Delta) - 26.8 \qquad (11)$$

These must be taken as amplitudes in Papeete harbor; for other receiving sites, local bathymetry entices additional corrections, which, for example, can reach a factor of 3 for resonant bays in the Marquesas chain. The upper bound (dashed line on Fig. 1) is related to a couple of events in the 10^{28} dyne-cm range, and may not be realistically extrapolated to extremely large moments. We interpret it as an absolute maximum for events with $M_m \leqq 9$.

Risk Levels as a Function of M_0

In establishing seismic thresholds for tsunami warning, we assume that tsunami risk is substantial when the upper bound on the peak-to-peak amplitude predicted at PPT (equation 9) reaches 1 m. Data from Figure 1, as well as the compilation of historical references (e.g., Pararas-Carayannis, 1977; Solov'iev and Go, 1984), suggests the following criteria for substantial tsunami risk: $M_0 \geqq 5 \times 10^{28}$ dyne-cm for Samoa-Tonga-Kermadec epicenters, and $M_0 \geqq 10^{29}$ dyne-cm for all other epicenters. The former figure, obtained here experimentally, is in agreement with Ward's (1980) theoretical threshold for destructive tsunamis. We treat separately the case of epicenters from the region Samoa-Tonga-Kermadec, which can be as close as 22° from PPT; for such events, geometrical spreading is significantly reduced, resulting in substantial distance corrections in (9 through 11).

In this framework, the following risk levels have been identified as a function of the magnitude M_m:

1. $M_m < 7$ ($M_0 < 10^{27}$ dyne-cm): No tsunami risk.
2. $7 \leqq M_m < 8$ ($10^{27} \leqq M_0 < 10^{28}$ dyne-cm): The generation of a very large tsunami remains improbable, but a "tsunami earthquake" cannot be totally ruled out. Although it may be improper to describe it in terms of M_m or M_0, the Aleutian earthquake-landslide of 1 April 1946 apparently belonged to this range of seismic measurements (Kanamori, 1972), and yet it created one of the two largest tsunamis in the past 150 yr. Further interpretation, for example of T-wave durations, may be warranted.
3. $8 \leqq M_m < 8.7$ ($10^{28} \leqq M_0 < 5 \times 10^{28}$ dyne-cm): A tsunami will probably be generated, but except for the possible case of a tsunami earthquake, should not be catastrophic at teleseismic distances from the epicenter. Interpret T waves.
4. $8.7 \leqq M_m < 9.3$ ($5 \times 10^{28} \leqq M_0 < 2 \times 10^{29}$ dyne-cm): Probable generation of a potentially destructive tsunami. Immediate tsunami watch issued if epicenter is in Samoa-Tonga-Kermadec, or otherwise closer than 4000 km.

5. $M_m \geqq 9.3$ ($M_0 \geqq 2 \times 10^{29}$ dyne-cm): Generation of a very large, probably very destructive tsunami. Immediate alarm issued for Samoa-Tonga-Kermadec epicenters; immediate tsunami watch issued for other regions.

The following are definitions of "Tsunami Watch" and "Tsunami Alarm" as they are used by CPPT: A *Tsunami Watch* is a first-level warning, designed to acquaint Civil Defense authorities of the possibility of a substantial tsunami, in order to allow them to achieve readiness in case of the later issuance of a tsunami alarm. A tsunami watch issued by CPPT includes predicted arrival times of the wave in Polynesia. A *Tsunami Alarm* warrants immediate action on the part of Civil Defense authorities, in compliance with relevant governmental procedures. In most cases, it will follow a tsunami watch, but could be issued early in the case of close-by epicenters. The tsunami alarm confirms arrival times at Polynesian islands.

Obviously, our estimate of tsunami risk is later updated, taking into account tidal gauge data, as they become available following propagation of the tsunami wave, through retransmission to CPPT by the Pacific Tsunami Warning Center in Honolulu, and from the HANDAR GEOS platforms at Rarotonga (Cook Islands), Nuku-Hiva (Marquesas Islands), Easter Island, and, in the near future, Niue Island.

Automation of the Measurements

In this section, we discuss briefly an algorithm allowing for automation of the measurement of M_m, which is now used routinely by CPPT. Automated measurements have long been implemented for conventional magnitude scales, notably for the study of regional seismicity.

Our algorithm is based on the following steps: First, a strong event detector is triggered, based on the use of 11 short-period stations in the 350-km aperture Polynesian array continuously telemetered to PPT (see for example Talandier and Kuster (1976)), and a classic multiple criterion of amplitude threshold, frequency content, duration, and simultaneity. Next, an automated locator uses P times across the array to estimate an epicentral region and an arrival window for R_1. Okal and Kuster (1975) have shown that the use of stations on both Rangiroa and the Society Islands protects against the possible bias due to local receiver structure on slowness vectors derived from short-period first arrival times. In order to further guard against this effect, we obtain an independent estimate of the location from three-component long-period records at a single station (PPT), by retrieving the back-azimuth from the polarity of the three components of the P wave, and distance from the S-P time interval. After the location is obtained, the process triggers acquisition into the computer of 819.2 sec at a 0.2 sec sampling rate. The computation of M_m then proceeds in two independent ways, providing redundancy of the final results:

Frequency-Domain Measurement

The time series is simply run through a standard FFT algorithm and the correction C_S applied at each FFT frequency between 50 sec and 300 sec. C_D is computed by splitting the path into "pure" segments, and applying the adequate attenuation factors. M_m is then computed from equation (3) at the various periods, and the largest value retained.

Time-Domain Measurement

The signal is run through an analog bandpass filter, eliminating periods outside the 50 to 300 sec range. The resulting time series (Fig. 7) is searched for subsequent

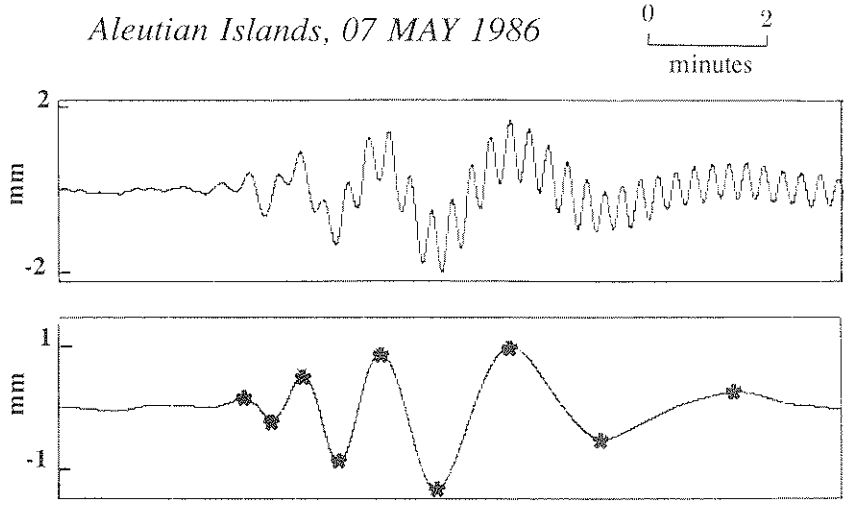

FIG. 7. Principle of automatic determination of time-domain magnitude. *Top*: Original record of 7 May 1986 Aleutian event at PPT. *Bottom*: Same record after filtering out periods greater than 50 sec. The stars indicate the automatic picks of peaks and troughs, from which the amplitudes and periods are estimated for use in (5).

maxima and minima reaching at least 10 per cent of the absolute maximum amplitude of the signal; the resulting amplitudes and periods of the corresponding arches are retained. For each of them, M_m is computed through equation (5) and the maximum value retained.

Once these estimates of M_m are obtained, and for both of them, the computer prints out automatically estimates of tsunami heights (equations (9) through (11)) and arrival times at various Polynesian sites. On the basis of these results, and if necessary of an interpretation of T waves, a geophysicists (on call 24 hr a day) has the ultimate responsibility of issuing a tsunami watch or alarm.

CONCLUSIONS

1. The mantle magnitude M_m developed by Okal and Talandier (1987, 1989) and Talandier *et al.* (1987) allows recovery of the seismic moment of teleseismic Pacific earthquakes with a standard deviation on the order of ± 0.2 units of magnitude.
2. Estimates of expected tsunami heights for Papeete can be reliably derived from the measurement of M_m, and hence M_0. When completed by such effects as known resonant factors for harbors and bays and high seas focusing due to lateral heterogeneity in bathymetry, this approach can easily be generalized to other Pacific sites.
3. The more easily taken time-domain measurements show no significant difference with frequency domain estimations; they can be extended down to $M_0 = 5 \times 10^{24}$ dyne-cm, while keeping the same constants in the equation (5) defining $M_m{}^{TD}$. The possibility of using time-domain records means that the method can be used even in the absence of computing facilities, once a chart of the corrections C_D has been prepared for a given observatory, as a function of frequency and for all potentially active epicentral areas.

The major limitation of the proposed method regards the so-called "tsunami earthquakes" (Kanamori, 1972; Fukao, 1979), which can be defined as events whose

tsunamis are significantly greater than would be expected from their seismic waves. This definition carries in itself the impossibility to effect a proper warning based on seismic waves. Examples of tsunami earthquakes are the 1975 Nemuro-Oki, 1963 (20 October) Kurile, and 1982 Tonga events; also, the 1946 Aleutian earthquake-landslide falls in this general category. One could in principle guard against tsunami earthquakes by reducing considerably (in practice by one order of magnitude) the thresholds for the issuance of tsunami watches or alarms. Because of the rarity of tsunami earthquakes, this would lead to a large number of false alarms (conceivably several per year), thereby defeating the very purpose of tsunami warning, i.e., obtaining a realistic estimate of expectable tsunami amplitudes. In Okal (1988), we have discussed several parameters whose influence has been suggested as responsible for such events, and concluded that they probably involve rupture propagating into sedimentary material of significantly weaker than normal mechanical properties. The recovery of this behavior in real time remains a challenge. In particular, a detailed study of the 1982 Tonga event (P. R. Lundgren *et al.*, manuscript in preparation) shows that this earthquake does not feature an anomalous behavior of its seismic moment rate function at ultra-low frequencies. Similar conclusions were reached by Fukao (1979), regarding the 1963 and 1975 events.

Finally, we wish to emphasize that while this method was being developed, we were able to obtain a correct estimate of $M_0 = 1.0 \times 10^{28}$ dyne-cm for the Aleutian event of 7 May 1986 (Fig. 7), within a little more than 2 hr of the origin time. As a result, no tsunami warning was issued for French Polynesia, and a false alarm avoided (Talandier *et al.*, 1986), while an estimate of tsunami danger for the same event based primarily on M_s resulted in the unnecessary evacuation of thousands of residents of Hawaii, Oregon, and Washington. We wish to stress that while the final decision on such matters as evacuation of low-lying areas, and implementation of emergency procedures is clearly the responsibility of governmental agencies, the scientific community has the duty of providing the latter with the best *quantitative* information possible. We believe that the use of M_m, and of formulas such as (9) through (11), which are fully justifiable from a theoretical point of view, and have been verified against experimental datasets, represents significant progress in this direction.

ACKNOWLEDGMENTS

We thank Domenico Giardini for a copy of the Harvard CMT dataset, and Barbara Romanowicz for preliminary estimates of M_0 for recent events. Discussions with Seth Stein and Otto Nuttli are also acknowledged. This research was supported by Commissariat à l'Energie Atomique (France), and the National Science Foundation, under grants EAR-84-05040 and EAR-87-20549.

REFERENCES

Abe, K. (1972). Mechanism and tectonic implications of the 1966 and 1970 Peru earthquakes, *Phys. Earth Planet. Interiors* **5**, 367–379.

Abe, K. (1973). Tsunami and mechanism of great earthquakes, *Phys. Earth Planet. Interiors* **7**, 143–153.

Aki, K. (1967). Scaling law of seismic spectrum, *J. Geophys. Res.* **72**, 1217–1231.

Canas, J. A. and B. J. Mitchell (1978). Lateral variation of surface-wave anelastic attenuation across the Pacific, *Bull. Seism. Soc. Am.* **68**, 1637–1650.

Dewey, J. W. and W. Spence (1979). Seismic gaps and source zones of recent large earthquakes in coastal Peru, *Pure Appl. Geophys.* **117**, 1148–1171.

Dziewonski, A. M. and J. H. Woodhouse (1983). An experiment in systematic study of global seismicity: centroid-moment tensor solutions for 201 moderate and large earthquakes in 1981, *J. Geophys. Res.* **88**, 3247–3271.

Dziewonski, A. M., A. Friedman, D. Giardini, and J. H. Woodhouse (1983). Global seismicity of 1982: centroid moment tensor solutions for 308 earthquakes, *Phys. Earth Planet. Interiors* **33**, 76–90.

Dziewonski, A. M., J. E. Franzen, and J. H. Woodhouse (1985). Centroid moment-tensor solutions for January–March 1985, *Phys. Earth Planet. Interiors* **40,** 249–258.

Dziewonski, A. M., J. E. Franzen, and J. H. Woodhouse (1986). Centroid moment-tensor solutions for July–September 1985, *Phys. Earth Planet. Interiors* **42,** 205–214.

Dziewonski, A. M., G. Ekström, J. E. Franzen, and J. H. Woodhouse (1987a). Global seismicity of 1979: centroid moment tensor solutions for 524 earthquakes, *Phys. Earth Planet. Interiors* **48,** 18–46.

Dziewonski, A. M., G. Ekström, J. E. Franzen, and J. H. Woodhouse (1987b). Centroid moment-tensor solutions for April–June 1986, *Phys. Earth Planet. Interiors* **45,** 229–239.

Dziewonski, A. M., G. Ekström, J. H. Woodhoouse, and G. Zwart (1987c). Centroid moment-tensor solutions for October–December 1986, *Phys. Earth Planet. Interiors* **48,** 5–17.

Dziewonski, A. M., G. Ekström, J. E. Franzen, and J. H. Woodhouse (1988). Global seismicity of 1981: centroid moment tensor solutions for 542 earthquakes, *Phys. Earth Planet. Interiors* **50,** 155–182.

Erdélyi, A. (1956). *Asymptotic Expansions*, Dover, New York, 108 pp.

Fukao, Y. (1979). Tsunami earthquakes and subduction processes near deep-sea trenches, *J. Geophys. Res.* **84,** 2303–2314.

Geller, R. J. (1976). Scaling relations for earthquake source parameters and magnitudes, *Bull. Seism. Soc. Am.* **66,** 1501–1523.

Gilbert, J. F. (1971). Excitation of the normal modes of the Earth by earthquake sources, *Geophys. J. Roy. Astr. Soc.* **22,** 223–226.

Harkrider, D. G. (1964). Surface waves in multilayered elastic media. I. Rayleigh and Love waves from buried sources in a multilayered half-space, *Bull. Seism. Soc. Am.* **54,** 627–679.

Hwang, H.-J. and B. J. Michell (1987). Shear velocities, Q_β, and the frequency dependence of Q_β in stable and tectonically active regions from surface wave observations, *Geophys. J. Roy. Astr. Soc.* **90,** 575–613.

Kanamori, H. (1970a). Synthesis of long-period surface waves and its application to earthquake source studies—Kurile Islands earthquake of October 13, 1963, *J. Geophys. Res.* **75,** 5011–5027.

Kanamori, H. (1970b). The Alaska earthquake of 1964: radiation of long-period surface waves and source mechanism, *J. Geophys. Res.* **75,** 5029–5040.

Kanamori, H. (1971). Focal mechanism of the Tokachi-Oki earthquake of May 16, 1968: contortion of the lithosphere at the junction of two trenches, *Tectonophysics* **12,** 1–13.

Kanamori, H. (1972). Mechanism of tsunami earthquakes, *Phys. Earth Planet. Inter.* **6,** 346–359.

Kanamori, H. (1977). The energy release in great earthquakes, *J. Geophys. Res.* **82,** 2981–2987.

Kanamori, H. and D. L. Anderson (1975a). Theoretical basis of some empirical relations in seismology, *Bull. Seism. Soc. Am.* **65,** 1073–1095.

Kanamori, H. and D. L. Anderson (1975b). Amplitude of the Earth's free oscillation and long-period characteristics of the earthquake source, *J. Geophys. Res.* **80,** 1075–1078.

Kanamori, H. and G. S. Stewart (1976). Mode of strain release along the Gibbs Fracture Zone, Mid-Atlantic Ridge, *Phys. Earth Planet. Inter.* **11,** 312–332.

Lundgren, P. R. and E. A. Okal (1988). Slab decoupling in the Tonga arc: the 22 June 1977 earthquake, *J. Geophys. Res.* **93,** 11355–11366.

Mitchell, B. J. and G.-K. Yu (1980). Surface-wave dispersion, regionalized velocity models, and anisotropy of the Pacific crust and upper mantle, *Geophys. J. Roy. Astr. Soc.* **63,** 497–514.

Monfret, T. and B. Romanowicz (1986). Importance of on-scale observations of first arriving Rayleigh wavetrains for source studies: example of the Chilean event of March 3, 1985 observed on the GEOSCOPE and IDA networks, *Geophys. Res. Lett.* **13,** 1015–1018.

Nakanishi, I. (1981). Shear velocity and shear attenuation models inverted from the world-wide and pure-path average data of mantle Rayleigh waves ($_0S_{25}$ to $_0S_{80}$) and fundamental spheroidal modes ($_0S_2$ to $_0S_{24}$), *Geophys. J. Roy. Astr. Soc.* **66,** 83–130.

Okal, E. A. (1988). Seismic parameters controlling far-field tsunami amplitudes: a review, *Natural Hazards Journal* **1,** 69–96.

Okal, E. A. (1989). A theoretical discussion of time-domain magnitudes: the Prague formula for M_s and the mantle magnitude M_m, *J. Geophys. Res.* **94** (in press).

Okal, E. A. and G. Kuster (1975). A teleseismic array study in French Polynesia: implications for local and distant structures, *Geophys. Res. Lett.* **2,** 5–8.

Okal, E. A. and J. Talandier (1986). *T*-wave duration, magnitudes and seismic moment of an earthquake: application to tsunami warning, *J. Phys. Earth* **34,** 19–42.

Okal, E. A. and J. Talandier (1987). M_m: theory of a variable-period mantle magnitude, *Geophys. Res. Lett.* **14,** 836–839.

Okal, E. A. and J. Talandier (1989). M_m: A variable period mantle magnitude, *J. Geophys. Res.* **94** (in press).

Pararas-Carayannis, G. (1977). *Catalogue of Tsunamis in Hawaii,* World Data Center, NOAA, Boulder, Colorado, 24–43.

Romanowicz, B. A. and P. Guillemant (1984). An experiment in the retrieval of depth and source mechanism of large earthquakes using very long-period Rayleigh wave data, *Bull. Seism. Soc. Am.* **74,** 417–437.

Saito, M. (1967). Excitation of free oscillations and surface waves by a point source in a vertically heterogeneous Earth, *J. Geophys. Res.* **72,** 3689–3699.

Shimazaki, K. (1974). Nemuro-Oki earthquake of June 17, 1973: a lithospheric rebound at the upper half of the interface, *Phys. Earth Planet. Inter.* **9,** 314–327.

Solov'iev, S. L. and Ch. N. Go (1984). *Catalogue of Tsunamis of the Pacific Ocean,* Canadian Translations of Fisheries and Aquatic Sciences 5077–5078, 2 Vol., Sidney, 722 pp.

Talandier, J. (1966). Contribution à la prévision des tsunamis, *C.R. Acad. Sci. Paris* **263B,** 940–942.

Talandier, J. (1972). Étude et prévision des tsunamis en Polynésie Française, *Thèse d'Université,* Université Pierre-et-Marie Curie, Paris, 128 pp.

Talandier, J. and G. T. Kuster (1976). Seismicity and submarine volcanic activity in French Polynesia, *J. Geophys. Res.* **81,** 936–948.

Talandier, J., E. A. Okal, and D. Reymond (1986). Mantle magnitude M_m: a new approach for the rapid estimation of seismic moments; application to the 1986 Aleutian earthquake (abstract), *EOS* **67,** 1081.

Talandier, J., D. Reymond, and E. A. Okal (1987). M_m: Use of a variable-period mantle magnitude for the rapid one-station estimation of teleseismic moments, *Geophys. Res. Lett.* **14,** 840–843.

Ward, S. N. (1980). Relationships of tsunami generation and an earthquake source, *J. Phys. Earth* **28,** 441–474.

Woods, M. T. and E. A. Okal (1987). Effect of variable bathymetry on the amplitude of teleseismic tsunamis: a ray-tracing experiment, *Geophys. Res. Lett.* **14,** 765–768.

LABORATOIRE DE GÉOPHYSIQUE
COMMISSARIAT À L'ENERGIE ATOMIQUE
AND CENTRE POLYNÉSIEN DE PRÉVENTION DES TSUNAMIS
BOÎTE POSTALE 640
PAPEETE, TAHITI, FRENCH POLYNESIA
(J.T.)

DEPARTMENT OF GEOLOGICAL SCIENCES
NORTHWESTERN UNIVERSITY
EVANSTON, ILLINOIS 60208
(E.A.O.)

Manuscript received 22 September 1988